Application of Passive SAW Resonant Sensors to Contactless Measurement of the Output Engine Torque in Passenger Cars

V. Kalinin, R. Lohr, A. Leigh, G. Bown
Transense Technologies plc
Bicester, Oxfordshire, UK

***Abstract* — An engine output torque measurement system employing 433 MHz SAW resonators as sensing elements is presented. Either one or two SAW sensing elements incorporating three or five one-port resonators are attached to a flexplate that couples the crankshaft to the torque converter of a car with automatic transmission. An optimum design of the flexplate is described that minimizes the influence of extraneous mechanical forces. Design of the large diameter RF rotary coupler, as well as torque and temperature calibration characteristics of the sensor, is presented. An interrogation algorithm and its influence on system bandwidth are discussed. Experimental results of dynamic tests characterizing accuracy of the torque measurement are presented.**

I. INTRODUCTION

Modern passenger cars are equipped with engine management and transmission control systems that require information on the engine output torque as one of the input signals. At the moment this information is obtained indirectly from a number of sensors and an engine torque model [1]. As a result of production variance and engine wear the estimated torque value lacks accuracy. Direct torque measurement would be advantageous for improving both engine and transmission efficiency.

There are two viable types of contactless torque sensors that are sufficiently robust, do not require any local dc power source and can potentially be close coupled to the engine crankshaft. The first is based on the magneto-elastic effect [2] while the second employs one-port SAW resonators or SAW reflective delay lines. The first type is sensitive to gradients of magnetic field and requires a considerable area on the gearbox input shaft that is very often not available in the current design of the power train of passenger cars. On the contrary, SAW devices require much less space and can be positioned not only on a shaft but also on a disk component within the powertrain e.g., in the case of automatic transmission, on the flexplate that connects the crankshaft to the torque converter. The paper is devoted to the development of the contactless flexplate torque sensor based on the backscattering of the RF signal from SAW resonators.

In a number of previous publications, both SAW reflective delay lines [3] and SAW resonators [4-7] have been used as passive sensing elements to measure torque on various shafts. Initially the resonant torque sensor contained two one-port resonators on two separate substrates made of ST-cut quartz that were directly bonded to the shaft at ±45° to the shaft axis [4]. Later, both resonators were made on a single Y+34° cut quartz substrate which allowed an increase in torque sensitivity and a reduction in its variation with temperature [5]. In order to cancel the influence of shaft bending on torque reading, one more sensing element was attached to the opposite side of the shaft. Since the number of resonators in the sensor increased from two to four it was decided to use sequential pulsed interrogation of the sensor in the time domain [6] rather than a parallel interrogation of each resonator by its own frequency control loop [5]. At the next stage it was realized that a better compensation of the residual temperature variation of the offset and sensitivity was required. As a result, one more resonator was added to one of the sensing elements [7] that allowed an independent temperature measurement and provided excellent stability of the torque reading over the entire temperature range.

Development of the flexplate torque sensor has raised a number of new issues that are addressed in this paper. The first is the mechanical design of the flexplate as a torque transducer that is relatively insensitive to extraneous forces, couples and vibrations. The second is the design of a large-circumference (close to one wavelength) RF rotary coupler that links the SAW sensors and the electronic interrogation unit. The last problem is the selection of the resonant frequency measurement sequence and algorithm for torque calculation that provides the best suppression of the parasitic signals and an acceptable system bandwidth. The paper also presents static calibration data for the sensor and its dynamic test results.

II. DESIGN OF THE FLEXPLATE TORQUE TRANSDUCER

A. SAW Sensing Elements

There are two types of sensing elements that can be used in the flexplate torque sensor. The first, shown in Fig 1a, is a low-frequency (LFSAW) device containing two one-port resonators M3SAW and M4SAW with resonant frequencies $f_5 \approx 429$ MHz and $f_4 \approx 431$ MHz connected in parallel. The second shown in Fig 1b is a high-frequency SAW (HFSAW) device containing three one-port resonators TSAW, M2SAW and M1SAW with resonant frequencies $f_3 \approx 433$ MHz, $f_2 \approx 435$ MHz and $f_1 \approx 437$ MHz also connected in parallel. Both types of SAW device are made on Y+34° cut quartz with the X axis normal to the long side of the substrate. Detailed design and characteristics of the devices are presented in [6, 7]. The unloaded Q factor of the resonators is around 10000 and the series resonant impedance is close to 50 Ω.

1-4244-0647-1/07/$20.00 ©2007 IEEE

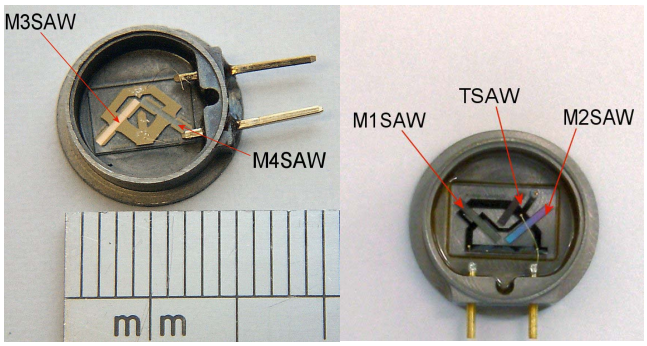

Figure 1. LFSAW sensing element (a) and HFSAW sensing element (b) without lids

If the sensing elements are subject to biaxial (shear) strain where $s_{xx} = s$, $s_{yy} = -s$ with the X axis of the substrate positioned at ±45° to the x and y co-ordinate axes then the difference frequencies $F_{m1} = f_1 - f_2$ and $F_{m2} = f_4 - f_5$ will change linearly with the strain s with a sensitivity of around 2.8 kHz/microstrain. By measuring F_{m1} and/or F_{m2} one can calculate the strain and find the torque M causing this strain.

Due to small differences in M1SAW (M3SAW) and M2SAW (M4SAW), complete temperature compensation for F_{m1} and F_{m2} is impossible. There is a residual temperature variation of the frequency differences at zero strain and the sensitivity also slightly varies with temperature. This variation can be taken into account in the sensor calibration model and cancelled out in the process of torque calculation in the digital signal processor (DSP) of the sensor interrogation unit (SIU). Information on temperature T is obtained by measuring one more frequency difference, $F_t = f_2 - f_3$ that has a sensitivity to temperature of around 2.1 kHz/°C.

Dependent on flexplate design and required level of suppression of parasitic extraneous forces and vibrations, one can use either the HFSAW alone or the LFSAW and HFSAW in combination.

B. Flexplate transducer

Lack of space for a shaft based torque sensor provides the opportunity to use the flexplate as the torque transducer. A typical production flexplate is a steel disk with diameter from 24 to 36 cm and thickness between 2 and 4 mm. On one side it is bolted to the crankshaft and on the other to the torque converter. A number of holes are usually stamped in the disk to make it lighter and provide the required compliance to absorb any small angular differences between the engine and transmission axes or axial movements due to loading on or within the torque converter. Therefore in general the flexplate will experience deformation not just due to applied torque but also due to out-of-plane bending, side and end loads.

Standard flexplate designs provide mechanical stiffness under torque and compliance under other loading conditions while meeting strict cost goals. However in order to provide a sensor position with sufficiently symmetrical distribution of a pure shear strain, even in the presence of extraneous forces and couples, a new or significantly modified flexplate design is required.

Fig. 2 shows a flexplate designed specifically as a torque transducer for the case of 120° angle between the bolts connecting the flexplate to the torque converter. It makes sense to use only one

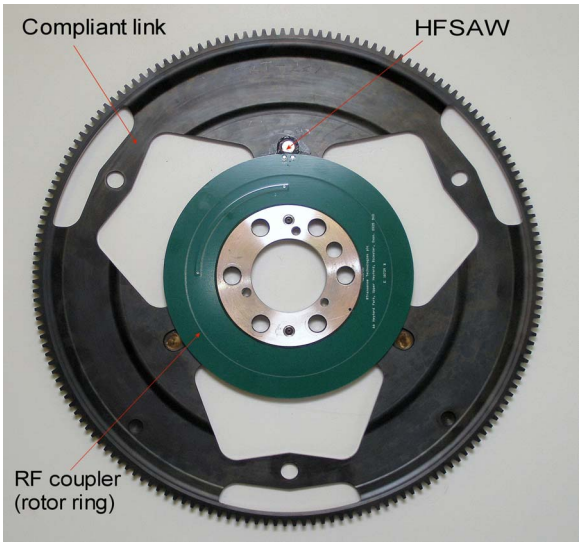

Figure 2. Flexplate with a single sensing element and a rotor ring of the RF coupler

sensing element, HFSAW, in this case. A second element would not further reduce parasitic signals due to its asymmetric position relative to the HFSAW and the flexplate centre. The following considerations are taken into account while selecting the shape and the size of the holes as well as position for the sensing element:

(a) The sensor is attached in an area of essentially uniform shear strain due to torque and placed symmetrically relative to the bolts connecting the flexplate to the torque converter which reduces the influence of extraneous forces and couples.

(b) A significant reduction in the influence of bending is achieved by positioning the base of the sensing element not on the surface of the flexplate but buried at a certain depth corresponding to the local "neutral axis" of the flexplate.

(c) The flexplate is bolted to the torque converter at places that are connected to the rest of the flexplate through specially designed "compliant links" further reducing the influence of any angular misalignment between the crankshaft and the torque converter axes on the strain in the vicinity of the sensor.

(d) The detail shape of the large cutouts and plate thickness is optimised using FEA to achieve an appropriate shear strain level while ensuring the peak Von Mises stress is low enough to not introduce fatigue issues.

(e) The strain at the sensor location is close to s = 100 microstrain at the maximum torque value M_{max}. If torque varies from –800 Nm to +800 Nm, for instance, then it gives a torque sensitivity of $S_M = F_{m1,2}/M \approx 0.35$ kHz/Nm. The variation of the difference $F_{m1,2}$ due to torque is ±280 kHz. Since the standard deviation of the measured value of $F_{m1,2}$ is σ_F = 300-450 Hz [6, 7] one can estimate the resolution of the torque sensor $\delta_M = 3\sigma_F/(2S_M M_{max}) < 0.25\%$ FS. This is sufficient for the applications under consideration and provides more than 15-fold overload protection.

It is well-known that the value $F_m = (F_{m1} + F_{m2})/2$ is insensitive to bending if two sensing elements are attached to the opposite sides of a shaft [6]. A similar approach can be used for a flexplate with 90° angle between the bolts connecting the flexplate

to the torque converter: a proper orientation and diametrically opposite positioning of HFSAW and LFSAW provides efficient cancelling of a parasitic signal due to bending.

C. Design of a rotary RF coupler

Contactless connection between the rotating flexplate and the stationary SIU is provided by the rotary RF coupler based on coupled annular microstrips positioned on the rotor and the stator printed circuit boards in the form of rings.

The main function of the RF coupler is to ensure efficient transfer of RF power and a minimum variation of the measured frequency of the SAW response with the rotation angle. This issue was discussed in detail in [5] in application to an EPAS (electrical power assisted steering) torque sensor. An alternative design of the coupler with a smaller angular frequency variation was suggested in [8]. However, these types of split-ring couplers work well only if their circumference is smaller than half a wavelength which is typical for most of the shafts in a vehicle. The size of the flexplates is such that the circumference of the coupler is close to one wavelength. In this case, either the amplitude of the SAW response at the stator input is insufficient for reliable measurement at certain angles or the angular variation of the measured frequency is too big (up to 200 kHz).

A new proposed design of a large-diameter RF rotary coupler [9] also employs coupled annular 50Ω microstrip lines. However, unlike the couplers presented in [5, 8], the end of the stator microstrip is not short-circuited or open-circuited but terminated with a matched load. This ensures uniform distribution of the RF signal amplitude around the stator. A crucial requirement in the new design is the circumference being equal to an integer number of wavelengths thus preventing phase discontinuity at the stator feeding point. The rotor microstrip line is just a quarter-wave segment (see Fig 2) short-circuited at the end opposite to the rotor output where the sensing element is connected.

Simulations and experiments show that the variation of the peak power spectral density of the SAW response received by the SIU through the coupler with the rotation angle does not exceed 2%. Measured resonant frequency variation with the angle depends on the gap between the stator and the rotor. It is up to 4 kHz at a gap of 0.685 mm but less than 2 kHz for gaps above 1.3 mm. Since the character of the angular variation for all resonant frequencies is similar, the difference frequency variation is considerably smaller and does not exceed 600 Hz as shown in Fig. 3.

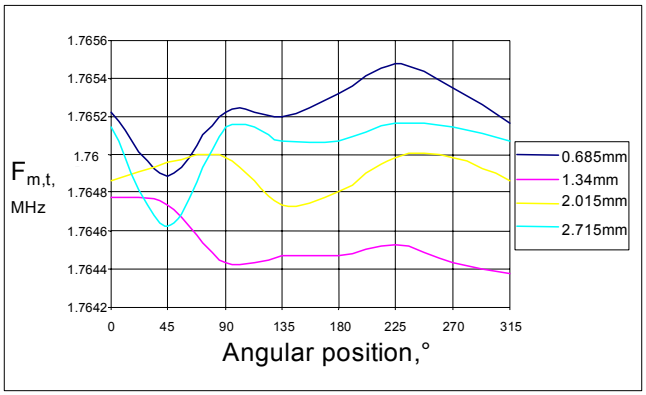

Figure 3. Typical variation of the measured frequency difference $F_{m,t}$ with the rotation angle at various gaps

III. Interrogation of the Flexplate Torque Sensor

A. Interrogation method

Contactless measurement of the SAW resonant frequencies is performed in the time domain by 3 us RF pulses with -7 dBm peak power. All three or five frequencies are measured sequentially to simplify and hence cost reduce the interrogation electronics. The method of interrogation is described in detail in [6]. The SIU is based on MLX11006 RF ASIC and TMS320F2801 DSP chip; its block diagram is presented in [9]. The frequency is measured by means of Fourier analysis of five coherently accumulated SAW responses, which takes $\tau = 250$ us per resonator.

B. Interrogation algorithm for HFSAW

Only three frequencies, $f_{1,2,3}$, need to be measured to find torque M and temperature T if there is one sensing element on the flexplate. One can suggest two possible interrogation schemes illustrated by the diagrams A and B in Fig. 6. Frequencies $f_{1,2}$ are measured alternately with the interval τ while the frequency of TSAW, f_3, is measured only once per $N\tau$ interval where $N = 3, 5, 7\ldots$, because T varies with time much slower than M. In practice $N \approx 500$ is sufficient to follow variation of temperature. Straight red lines in Fig. 4 mean calculation of the frequency differences $F_{m1,2}$ and F_t, black and red arrows mark the moments of updating values of torque and temperature respectively. The whole interrogation pattern is repeated with the period $N\tau$.

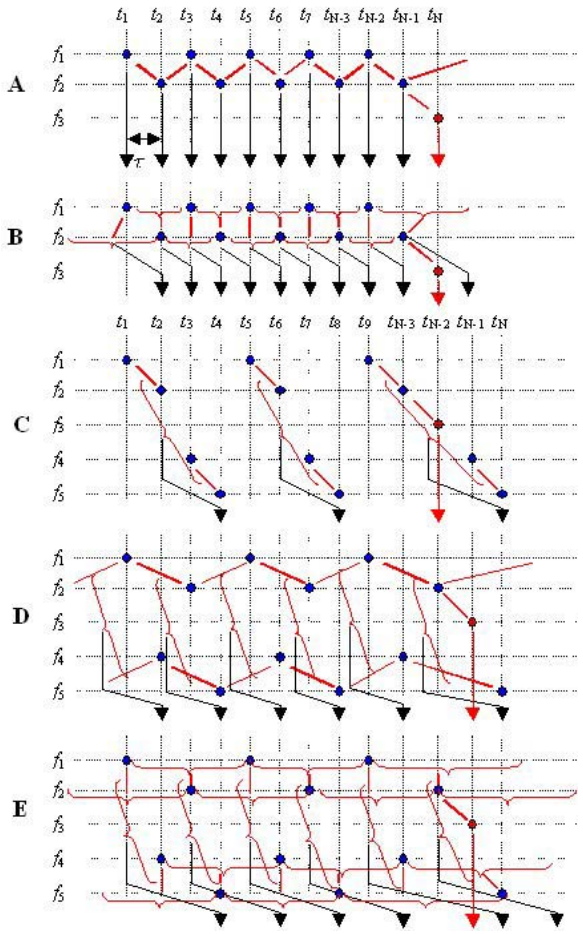

Figure 4. Interrogation schemes for one and two sensing elements

One can see that the scheme A has a latency τ and allows updating of torque with the period τ although it can also be updated with the period 2τ without affecting the system bandwidth B. The latter is entirely determined by the fact that the torque is effectively averaged over the period of τ due to sequential interrogation of M1SAW and M2SAW. The simulated system frequency response (ratio of the measured torque amplitude to the actual torque amplitude against the frequency F of the applied sinusoidal torque) is shown in Fig. 5. The 3 dB system bandwidth is B = 1 kHz and aliasing effect takes place at F > 2 kHz.

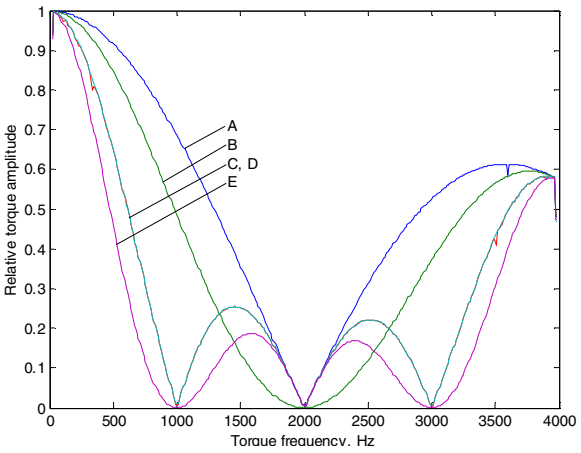

Figure 5. Simulated system frequency response for different interrogation schemes

Apart from torque, the sensing element is also subject to various parasitic mechanical forces that can be regarded as interference signals. Due to symmetric and orthogonal position of the resonators on the flexplate, one can decompose all sorts of extraneous forces into common-mode and differential mode signals. A common-mode interference signal changes the frequencies of M1SAW and M2SAW in the same direction so it should be cancelled when F_{m1} is calculated. However it takes place only for a static interference. If the interference varies with time the suppression of the common-mode interference is not perfect because of sequential measurement of the frequencies f_1 and f_2. Fig. 6 shows that the measured interference level increases almost linearly with frequency (see curve A).

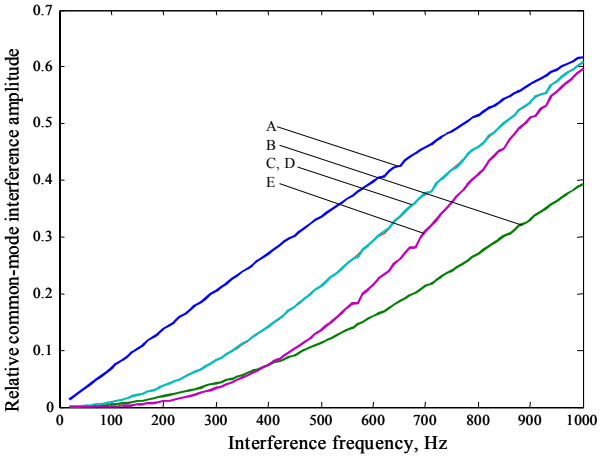

Figure 6. Suppression of the common-mode interference against its frequency for different interrogation schemes

Suppression of the common-mode interference can be significantly improved if the scheme B is used. Curve B in Fig. 6 illustrates this fact. The frequency difference F_{m1} is now calculated between $f_{1,2}(t_i)$ and $[f_{2,1}(t_{i-1}) + f_{2,1}(t_{i+1})]/2$ (figure brackets in Fig. 4 mean averaging). The price one has to pay for better suppression is the latency increased up to approximately 1.5τ and the system bandwidth reduced to B = 0.74 kHz (see curve B in Fig. 5).

As far as a differential-mode interference is concerned, one cannot cancel it using just a single sensing element because the interference changes the frequencies f_1 and f_2 in the opposite directions. Curves A and B in Fig. 7 showing the theoretically calculated level of suppression of the differential-mode interference against its frequency confirm it.

C. *Interrogation algorithm for HFSAW and LFSAW*

A proper orientation of the second sensing element, LFSAW, on the flexplate ensures that the torque changes the frequency differences F_{m1} and F_{m2} in the same direction while the differential-mode interference changes them in the opposite directions. As a result the interference is cancelled when the average frequency difference F_m is calculated.

The simplest sequential interrogation scheme for the two sensing elements is scheme C shown in Fig. 4 (N = 5, 9, 13…, in practice $N \approx 500$). It has the approximate latency 2τ and the torque updating period 4τ = 1 ms. Fidelity of the sampled torque signal can be improved if the updating period is halved, i.e. equals 2τ. This can be achieved in the scheme D with alternate calculation of the difference frequencies. Both schemes C and D have the same frequency response (see Fig. 5), B = 0.47 kHz, the same latency, and the same level of common-mode interference suppression (see Fig. 6). The scheme D though has a better suppression of the differential-mode interference (see Fig. 7) because the two averaged frequency differences are separated by the interval τ instead of 2τ as it is in the case of the scheme C.

Even better suppression of both interference modes is achieved in the scheme E also shown in Fig. 4. It implements averaging of the resonant frequencies similar to that used in the scheme B. Better suppression is achieved at the expense of the increase of the latency

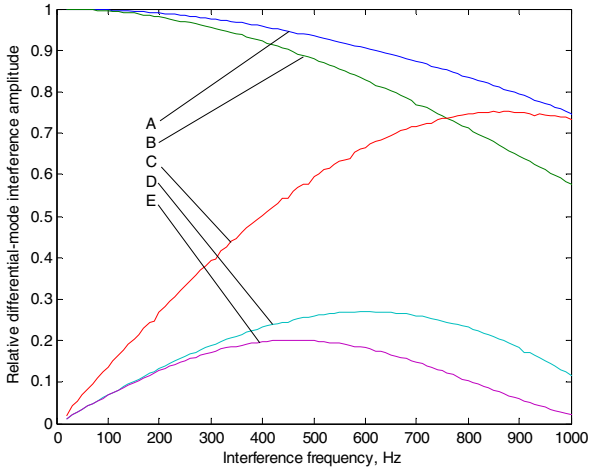

Figure 7. Suppression of the differential-mode interference against its frequency for different interrogation schemes

approximately up to 3τ and the bandwidth reduction down to B = 0.36 kHz.

Selection of the interrogation algorithm is dictated by the requirements on the bandwidth, latency and suppression of the unwanted signals. If only one sensing element is available then it makes sense to select the scheme A because it has a wider system bandwidth and the scheme B does not suppress the differential-mode interference anyway. If two sensing elements are installed then the scheme E is preferable for its best performance in the presence of extraneous mechanical forces and couples.

IV. Static Calibration Characteristics

The flexplate sensor, like the shaft sensor described in [5, 7], requires static calibration over the entire temperature range from -40° to +125°C. Fig. 8 shows static characteristics of a typical flexplate with two sensing elements measured within a slightly smaller range of torque and temperature. Variation of the averaged difference frequency F_m with torque at different temperatures is presented in Fig. 8a, while Fig. 8b shows thermal variation of F_t at different torque values. The mathematical model describing these characteristics is as follows [7]:

$$F_m = \begin{cases} S_p(T)M + F_0(T), & M \ge 0, \\ S_n(T)M + F_0(T), & M < 0 \end{cases} \quad (1)$$

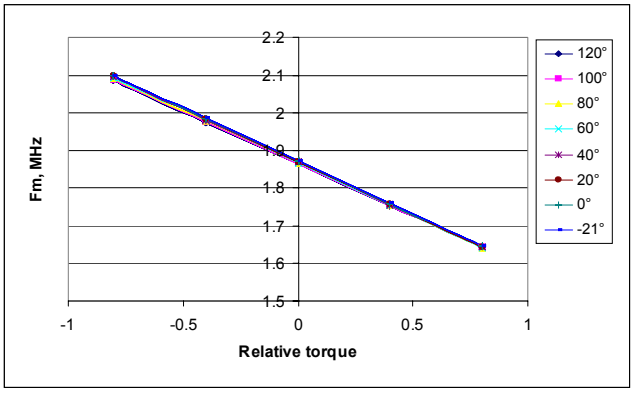

(a)

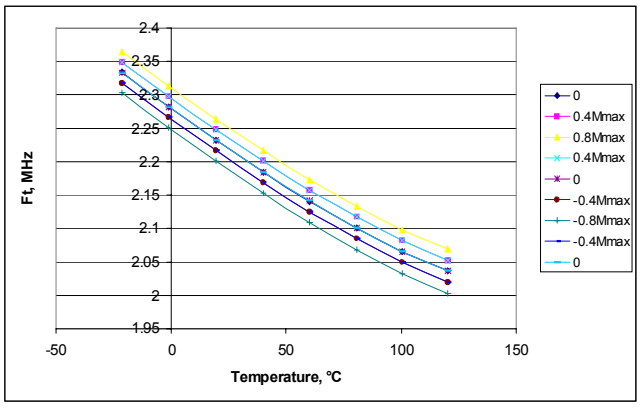

(b)

Figure 8. Calibration characteristics of a typical flexplate sensor: (a) F_m against M/M_{max} for different temperatures (b) F_t against temperaure for different torque values

$$F_t = 100a_1 - a_2T - 0.1a_3M + 0.001a_4T^2 + 10^{-5}a_5T^3 \quad (2)$$

where $F_0(T)$ is the offset as a function of temperature, $S_{p,n}(T)$ are positive and negative torque sensitivities as functions of temperature, and $a_{1\text{-}5}$ are calibration coefficients. All the model parameters are found by LMS curve fitting. Piecewise-linear approximation of F_m is used in order to minimise non-linearity of the sensor. Variations of the offset and the sensitivities with temperature are stored in the DSP memory in the form of look-up tables.

Eqs. (1)-(2) describe the calibration characteristics with the accuracy of around ±1 kHz that approximately corresponds to the temperature errors of ±0.5°C and the torque errors of 0.2% of the full scale.

Torque M and temperature T are calculated from the measured values of F_m and F_t by means of an iterative solution of Eqs. (1)-(2). Since the value of F_t is measured only once per N interrogation cycles as follows from the previous section, the values of M in the remaining N–1 cycles are calculated using just Eq. (1) and the previously measured value of T. In order to reduce the influence of mechanical forces on the measured temperature, a moving average of 64 previous T readings is used to find M from Eq. (1).

V. Dynamic Performance of the Flexplate Sensor

Flexplate sensors described in the previous sections were tested with real IC engines on test rigs equipped with dynamometers allowing to set up a certain value of the average torque M_{dyno}. The test software produced samples of an instantaneous torque measured with the period of 2τ = 0.5 ms according to schemes A and E. It also produced averaged temperature readings and torque values M_{ave} averaged over two rotations of the crankshaft.

Fig. 9 shows a typical variation of the instantaneous torque M with time measured by the flexplate with a single sensing element at the shaft rotation speed Ω = 3000 rpm, the average dyno torque M_{dyno} = 250 Nm and the engine temperature 90°C. One can clearly see individual firing pulses in the torque signal with the frequency 200 Hz. The spectrum of the torque signal presented in Fig. 10 does not contain any visible component due to bending at the rotation frequency 50 Hz but there are harmonics of the firing

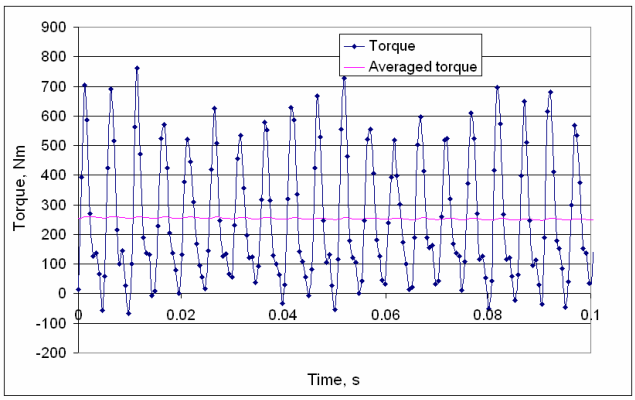

Figure 9. Variation of the instantaneous and averaged measured torque with time for a single-element flexplate sensor at Ω = 3000 rpm and M_{dyno} = 250 Nm.

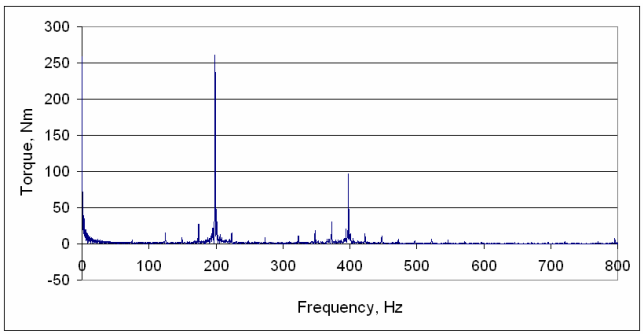

Figure 10. Figure 15. Spectrum of the instantaneous torque measured by a single-element flexplate sensor at Ω = 3000 rpm and M_{dyno} = 250 Nm.

frequency and the sidebands associated with the modulation of the firing pulses at half of the shaft rotation frequency. The error in measuring the average torque is only 4 Nm. The spectral component due to bending is visible at other speeds of rotation but it is quite small as a result of a proper mechanical design of the flexplate, e.g. it is only 6.4% of the amplitude of the 1st harmonic of the firing frequency at Ω = 1500 rpm.

Suppression of the parasitic signals is even better for the two-element flexplate sensor. Variation of the measured average torque M_{ave} with the applied torque M_{dyno} at various values of Ω for the two-element sensor is presented in Fig. 11. Linearity of the sensor characteristic is very good, the total error does not exceed 5 Nm, which is 1.5% of the full scale of M_{ave} for this sensor. It is mainly due to a small variation of the offset with the rotation speed, probably, due to a centrifugal force. The sensitivity variation with the rotation speed is less than ±1%.

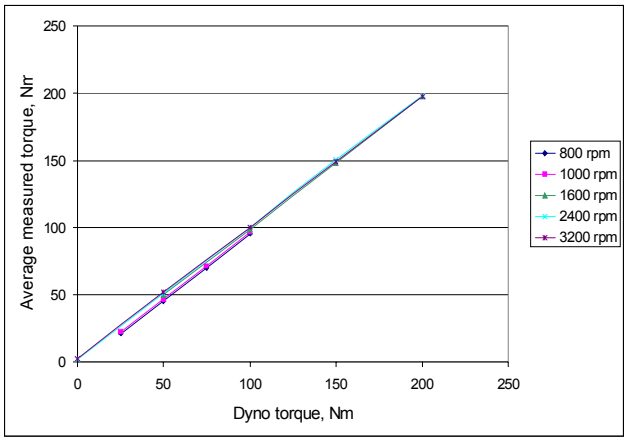

Figure 11. Average measured torque against the dyno torque for different speeds of rotation.

It is relatively easy to check the accuracy of measuring the average engine torque but it is more difficult to check how accurately the pulses observed in the instantaneous torque signal represent the actual contribution of the individual cylinders to the output torque. Their magnitude may be affected by engine vibrations and excitation of the vibrational modes of the flexplate, so this issue requires further investigation.

VI. Conclusions

A contactless sensor for measuring torque at the output of the IC engine of a car has been developed. The sensor consists of a flexplate with one or two sensing elements installed on it. Sensing elements contain either three or two one-port SAW resonators fabricated on a single quartz substrate and having resonant frequencies from 429 to 437 MHz. Mechanical design of the flexplate, position and orientation of the SAW resonators provides good cancellation of parasitic signals due to extraneous forces and couples. The calibration model of the sensor provides temperature compensation. Wireless interrogation of each resonator is performed sequentially in the time domain by the electronic unit containing only two main components – a DSP chip and a transceiver in the form of the RF ASIC. The signal is delivered to and from the sensor through the RF rotary coupler specially designed to minimize variation of the measured frequency with the rotation angle. The torque measurement algorithm ensures additional suppression of parasitic signals in the case of a flexplate with two sensing elements.

Dynamic tests of the flexplate sensors confirmed their good linearity and relatively small errors in the measured average torque below 1.5% of the full scale. This opens prospects of using the sensor in transmission control systems. The measured instantaneous torque signal contained information on the individual firing pulses that could also be used in future more sophisticated and accurate engine management systems.

Acknowledgement

The authors are grateful to John Beckley of Transense Technologies plc for numerous fruitful discussions.

References

[1] M. Ibamoto, H. Kuroiva, T. Minowa, K. Sato, T. Tsuchiya, "Development of smooth shift control system with output torque estimation", SAE Paper No. 950900, 1995.

[2] I. J. Garshelis, C. R. Conto, "A torque transducer utilizing a ring divided into two oppositely polarized regions", J. Appl. Phys. Vol. 79, No. 8, 1996, pp. 4756-4758.

[3] L. Reindl, G. Scholl, T. Ostertag, H. Scherr, U. Wolff, and F. Schmidt, "Theory and application of passive SAW radio transponders as sensors", IEEE Trans.Ultrason., Ferroelect., Freq. Contr., vol. 45, pp. 1281-1292, 1998.

[4] R. Grossmann, J. Michel, T. Sachs, E. Schrufer, "Measurement of mechanical quantities using quartz sensors", Proc. Europ. Freq. Time Forum, pp. 376-381, 5-7 March, 1996.

[5] J. Beckley, V. Kalinin, M. Lee, K. Voliansky, "Non-contact torque sensors based on SAW resonators", 2002 IEEE International Frequency Control Symp., pp. 202-213, May 2002.

[6] V. Kalinin, G. Bown, J. Beckley and R. Lohr, "Pulsed interrogation of the SAW torque sensor for electrical power assisted steering", Proc. IEEE Int. Ultrason., Ferroelectrics, and Freq. Control Joint 50th Anniversary Conf., pp. 1577-1580, 2004.

[7] V. Kalinin, G. Bown, A. Leigh. Contactless Torque and Temperature Sensor Based on SAW Resonators. Proc. IEEE Ultrason. Symp., pp. 1490-1493, 2006.

[8] J. Beckley, V. Kalinin, "Split-ring coupler incorporating dual resonant sensors", GB Applic. No. GB0409251.6, GB filing date: 15 April 2005.

[9] V. Kalinin, "Influence of receiver noise properties on resolution of passive wireless resonant SAW sensors". Proc. IEEE Ultrason. Symp., pp. 1452 – 1455, 2005.